Chen, Ruiying; Martin, Floran; Li, Yongjian; Yue, Shuaichao; Li, Yating; Belahcen, Anouar

Anisotropic Vector Hysteresis Modeling for Non-oriented Electrical Steel Sheets under Multiaxial Stress

Published in:
IEEE Transactions on Magnetics

DOI:
10.1109/TMAG.2024.3467696

Published: 01/01/2024

Document Version
Peer-reviewed accepted author manuscript, also known as Final accepted manuscript or Post-print

Please cite the original version:
Chen, R., Martin, F., Li, Y., Yue, S., Li, Y., & Belahcen, A. (2024). Anisotropic Vector Hysteresis Modeling for Non-oriented Electrical Steel Sheets under Multiaxial Stress. *IEEE Transactions on Magnetics*, *60*(12), Article 7301505. https://doi.org/10.1109/TMAG.2024.3467696

Anisotropic Vector Hysteresis Modeling under Multiaxial Stress

Ruiying Chen[1], Floran Martin[2], Yongjian Li[3], Shuaichao Yue[3], Yating Li[3] and Anouar Belahcen[2], *Senior Member, IEEE*

[1]Department of Electrical Engineering, Tsinghua University, Beijing 100190, China
[2]Department of Electrical Engineering and Automation, Aalto University, 00076 Espoo, Finland
[3]State Key Laboratory of EERI, Hebei University of Technology, Tianjin 300130, China

A model for predicting the vector hysteresis properties of non-oriented steel sheets under multiaxial stress is proposed. Based on the magneto-elastic energy of single crystal and coordinate transformation from crystal to sample, the effective field contains anisotropy and magneto-mechanical characteristics are derived. By combining the effective field with the energy-based model, the sensibility of mechanical stress is accounted for both the reversible and irreversible magnetization aspects. Comparisons between measured and calculated results are performed to validate the model. The results show that the model can accurately predict the rotational magnetic properties under multiaxial stress.

***Index Terms*—Magnetic anisotropy, magneto-elasticity, multiaxial stress, vector hysteresis.**

I. Introduction

The magnetic properties of core material are altered due to the application of significant mechanical stresses during the manufacturing processes of rotating electrical machines. These stresses are multiaxial and the core material works under the rotating field [1]. Consequently, it is important to propose a vector hysteresis model that can account for the influence of multiaxial stress to accurately predict the magnetic properties and loss of core material.

There are two typical methods to model the effect of multiaxial stress on magnetic properties. One is introducing an equivalent stress to transform the stress tensor into a scalar [2]. Based on this method, hysteresis models and measurements that account for uniaxial stress can be used directly to predict the magnetic properties under multiaxial stress [3]. Normally, the calculation process of that kind of model is simple and fast. However, ignoring the anisotropy caused by stress affects the accuracy of hysteresis model. Another is establishing macroscopic constitutive laws by a micro-mechanical description of magnetic domain structures, called the multiscale model [4]. Multiscale model has only several parameters but has wide applicability to different multiaxial stress conditions. The magneto-mechanical behaviors described by this model do not contain hysteresis characteristics. Therefore, it is necessary to combine it with other hysteresis models which separate the magnetization process into reversible and irreversible parts [5]-[6]. Meanwhile, multiscale model relies on microscopic measurements, which limits its application scope. Although its simplified version does not require microscopic measurements, the prediction accuracy is decreased.

Similar to the multiscale model, this paper benefits from the microscopic crystal energy theory to describe the macroscopic magnetic properties. Based on the anisotropic vector hysteresis model we proposed before [7], a term about multiaxial stress is further added to the expression of effective field and also changes the pinning field of hysterons. Only the macroscopic measurements are required to identify the model while a high accuracy is ensured. First, the effective field considering the magneto-static energy, anisotropy energy and magneto-elastic energy of the crystal is derived. Then, taking the effective field as input of the energy-based model and using the hysterons whose pinning field varies with the energy-related matrix to propose a vector hysteresis model under multiaxial stress. Finally, the proposed model is identified and validated by data of rotational magnetization under multiaxial stress.

II. Method

A. Effective Field under Multiaxial Stress

For a single cubic crystal with magnetization direction $\boldsymbol{\gamma}_c = [\gamma_1\ \gamma_2\ \gamma_3]^T$, its magnetostrictive strain $\boldsymbol{\varepsilon}_\lambda$ is:

$$\boldsymbol{\varepsilon}_\lambda = \frac{3}{2}\begin{bmatrix} \lambda_{100}\left(\gamma_1^2 - 1/3\right) & \lambda_{111}\gamma_1\gamma_2 & \lambda_{111}\gamma_1\gamma_3 \\ \lambda_{111}\gamma_2\gamma_1 & \lambda_{100}\left(\gamma_2^2 - 1/3\right) & \lambda_{111}\gamma_2\gamma_3 \\ \lambda_{111}\gamma_3\gamma_1 & \lambda_{111}\gamma_3\gamma_2 & \lambda_{100}\left(\gamma_3^2 - 1/3\right) \end{bmatrix} \quad (1)$$

where λ_{100} and λ_{111} are the saturation magnetostriction coefficients in the <100> and <111> directions of the cubic crystal, respectively.

When the planar multiaxial stress $\boldsymbol{\sigma}$ is applied

$$\boldsymbol{\sigma} = \begin{bmatrix} \sigma_{xx} & \tau_{xy} & 0 \\ \tau_{yx} & \sigma_{yy} & 0 \\ 0 & 0 & 0 \end{bmatrix} \quad (2)$$

If the crystal frame in (1) is converted to the sample frame, the magneto-elastic energy of crystal can be expressed as $W_{\sigma c} = -\boldsymbol{\sigma} : \boldsymbol{\varepsilon}_\lambda$. The volume changes of the materials in this study can be ignored, therefore

$$W_{\sigma c} = -\boldsymbol{\sigma}_{dev} : \boldsymbol{\varepsilon}_\lambda \quad (3)$$

The deviatoric part of the stress tensor $\boldsymbol{\sigma}_{\mathrm{dev}} = \boldsymbol{\sigma} - 1/3\mathrm{tr}(\boldsymbol{\sigma})\mathbf{I}$.

The sample can be treated as the assembly of cubic crystals. Define its anhysteretic magnetization as $\boldsymbol{M}_{\mathrm{anh}} = M_{\mathrm{anh}}\,\boldsymbol{e}_{\boldsymbol{M}\mathrm{anh}}$, $\boldsymbol{e}_{\boldsymbol{M}\mathrm{anh}} = [m_1\ m_2\ m_3]^{\mathrm{T}}$. The directions $\boldsymbol{\gamma}_{\mathrm{c}}$ of each crystal can be expressed in the sample coordinate system by a rotation matrix $\boldsymbol{R}$ and the following transformation:

$$\boldsymbol{\gamma}_{\mathrm{c}} = \boldsymbol{R}\cdot\boldsymbol{e}_{\boldsymbol{M}\mathrm{anh}} \tag{4}$$

Applying this transformation to (1), then the elements in $\boldsymbol{\varepsilon}_{\lambda}$ for two-dimensional (2D) condition ($m_3 = 0$) are

$$\begin{aligned}
\boldsymbol{\varepsilon}_{11} &= \lambda_{1120}m_1^2 + \lambda_{1102}m_2^2 + \lambda_{1111}m_1m_2\\
\boldsymbol{\varepsilon}_{22} &= \lambda_{2220}m_1^2 + \lambda_{2202}m_2^2 + \lambda_{2211}m_1m_2\\
\boldsymbol{\varepsilon}_{33} &= \lambda_{3320}m_1^2 + \lambda_{3302}m_2^2 + \lambda_{3311}m_1m_2\\
\boldsymbol{\varepsilon}_{12} &= \lambda_{1220}m_1^2 + \lambda_{1202}m_2^2 + \lambda_{1211}m_1m_2
\end{aligned} \tag{5}$$

In this equation, the subscript of ε represents the position in $\boldsymbol{\varepsilon}_{\lambda}$. Only the elements involved in the calculation of magneto-elastic energy are given, that is, the corresponding $\boldsymbol{\sigma}_{\mathrm{dev}}$ elements are not 0. The subscript of coefficient λ consists of the position of magnetostrictive strain element and the power of m_1 and m_2. It should be noted that the volume change is 0, so there is

$$\begin{aligned}
\lambda_{3320} &= -\lambda_{1120} - \lambda_{2220}\\
\lambda_{3302} &= -\lambda_{1102} - \lambda_{2202}\\
\lambda_{3311} &= -\lambda_{1111} - \lambda_{2211}
\end{aligned} \tag{6}$$

The elements of matrix $\boldsymbol{R}$ are contained in λ and do not need to be obtained. The sum of the magneto-elastic energy of crystals calculated by (3) in the sample gives the total magneto-elastic energy W_{σ}. The crystallographic texture is unknown, whereas W_{σ} still has the following form:

$$\begin{aligned}
-\frac{W_{\sigma}}{\mu_0 M_{\mathrm{S}}} &= \sigma_{xx}^{dev}(\lambda_{1120}m_1^2 + \lambda_{1102}m_2^2 + \lambda_{1111}m_1m_2)\\
&+ \sigma_{yy}^{dev}(\lambda_{2220}m_1^2 + \lambda_{2202}m_2^2 + \lambda_{2211}m_1m_2)\\
&+ \sigma_{zz}^{dev}(\lambda_{3320}m_1^2 + \lambda_{3302}m_2^2 + \lambda_{3311}m_1m_2)
\end{aligned} \tag{7}$$

where, μ_0 is the vacuum permeability and M_{s} the saturation magnetization of sample. Because τ_{xy} and τ_{yx} can not be applied in the rotational measurement system, their corresponding parts are omitted.

Similar to the relationship between the applied field $\boldsymbol{H}$ and the magneto-static energy W_{h} of single crystal, $W_{\mathrm{h}} = -\mu_0 m_{\mathrm{s}}\boldsymbol{H}\cdot\boldsymbol{\gamma}_{\mathrm{c}}$, the stress field $\boldsymbol{H}_{\sigma}$ is defined as

$$\boldsymbol{H}_{\sigma} = -\frac{1}{\mu_0 M_{\mathrm{S}}}\frac{\partial W_{\sigma}}{\partial \boldsymbol{e}_{\boldsymbol{M}\mathrm{anh}}} \tag{8}$$

However, the magnetostrictive coefficient λ is not a constant and is related to the magnitude of magnetization M and stress σ. In [8], λ is expressed as

$$\lambda = \lambda_0\left(\sum_{j=1}^{N_p} g_j M^{2j}\right)\left(q_1 + \tanh\left(\frac{q_2 - \sigma}{q_3}\right)\right) = \lambda_0 G(M)Q(\sigma) \tag{9}$$

where λ_0, g and q are parameters that need to be identified and M is the amplitude of magnetization. Although the above equation describes the uniaxial stress cases, the constant λ_{abcd} at each position in (7) can be modified to functions related to magnetization and stress based on this method. Firstly, λ0 in (9) is a constant, which can be directly replaced by λ_{abcd} in (7). Secondly, the deviatoric stress multiplied before λ_{abcd} will be used as a variable in function $Q(\sigma)$. Finally, replace M with $M_{\mathrm{an}}/M_{\mathrm{S}}$ as the variable for $G(M)$. Meanwhile, due to the presence of coercive field, the influence of stress on magnetic properties varies with the maximum magnetic density B_{p}. Therefore, term $(B_{\mathrm{p}}/2)^2$ is added to the expression of the stress field. In summary, the stress field under 2D condition can be expressed as:

$$\begin{aligned}
H_{\sigma x} &= \sum_{i=x,y,z} Q(\sigma_{ii}^{dev})\sigma_{ii}^{dev}(2\lambda_{ii20}m_1 + \lambda_{ii11}m_2)\\
H_{\sigma y} &= \sum_{i=x,y,z} Q(\sigma_{ii}^{dev})\sigma_{ii}^{dev}(2\lambda_{ii02}m_2 + \lambda_{ii11}m_1)
\end{aligned} \tag{10}$$

Combine the completed work in [7] and the above deduction, the expression of effective field $\boldsymbol{H}_{\mathrm{eff}}$ considering magnetic anisotropy and multiaxial stress is

$$\boldsymbol{H}_{\mathrm{eff}} = \boldsymbol{H} + F\left(\frac{M_{\mathrm{an}}}{M_{\mathrm{S}}}\right)\boldsymbol{H}_{\mathrm{an}} + \left(\frac{B_{\mathrm{p}}}{2}\right)^2 G\left(\frac{M_{\mathrm{an}}}{M_{\mathrm{S}}}\right)\boldsymbol{H}_{\sigma} \tag{11}$$

where $\boldsymbol{H}_{\mathrm{an}}$ is the anisotropic field. Vector anhysteretic magnetic properties can be predicted by the calculation of $\boldsymbol{H}_{\mathrm{eff}}$ and applying it to a scalar anhysteretic function. Detail of the definition of $\boldsymbol{H}_{\mathrm{eff}}$ and $F(M_{\mathrm{an}}/M_{\mathrm{s}})$, and the derivation process of $\boldsymbol{H}_{\mathrm{an}}$ can be found in [7].

B. Vector Hysteresis Model

To account for hysteresis, $\boldsymbol{H}_{\mathrm{eff}}$ is decomposed into reversible effective field $\boldsymbol{H}_{\mathrm{re\text{-}eff}}$ and irreversible field $\boldsymbol{H}_{\mathrm{ir}}$ in the frame of the energy-based (EB) model [9]

$$\boldsymbol{H}_{\mathrm{eff}} = \boldsymbol{H}_{\mathrm{re\text{-}eff}} + \boldsymbol{H}_{\mathrm{ir}} \tag{12}$$

$\boldsymbol{H}_{\mathrm{ir}}$ is predefined in the EB model by a series of hysteron with different pinning field h_{ir}. A two-dimensional matrix $\boldsymbol{k}$ is introduced to adjust the values of pinning field in different magnetization directions [10]

$$\boldsymbol{k} = \boldsymbol{k}_0 + k_{\mathrm{ani}}\left(\boldsymbol{K}_{\mathrm{an}} - W_0\mathbf{I}\right) + \boldsymbol{K}_{\sigma} \tag{13}$$

where k_{ani} is a constant, $\boldsymbol{k}_0$ is a constant matrix defined as [1 k_{12}^0

; k_{21}^0 k_{22}^0]$^{\mathrm{T}}$ and W_0 is the minimum value of anisotropy energy W_{an} [7]. The $W_0\mathbf{I}$ term is used to ensure the irreversible field is always positive. $\boldsymbol{K}_{\mathrm{an}}$ and $\boldsymbol{K}_{\sigma}$ are coefficient matrices corresponding to the $\boldsymbol{H}_{\mathrm{an}}$ and $\boldsymbol{H}_{\sigma}$ expressions, respectively.

Elements in $\boldsymbol{K}_{\mathrm{an}}$ are

$$\begin{aligned} k_{11}^{\mathrm{an}} &= K_{40}m_1^2 + K_{60}m_1^4 \\ k_{22}^{\mathrm{an}} &= K_{04}m_2^2 + K_{06}m_2^4 \\ k_{12}^{\mathrm{an}} &= k_{21}^{\mathrm{an}} = K_{22}m_1m_2 + K_{42}m_1^3m_2 + K_{24}m_1m_2^3 \end{aligned} \tag{14}$$

Elements in $\boldsymbol{K}_{\sigma}$ are

$$\begin{aligned} k_{11}^{\sigma} &= D_1(\sigma_{xx}^{\mathrm{dev}}\lambda_{1120} + \sigma_{yy}^{\mathrm{dev}}\lambda_{2220} + \sigma_{zz}^{\mathrm{dev}}\lambda_{3320}) \\ k_{22}^{\sigma} &= D_2(\sigma_{xx}^{\mathrm{dev}}\lambda_{1102} + \sigma_{yy}^{\mathrm{dev}}\lambda_{2202} + \sigma_{zz}^{\mathrm{dev}}\lambda_{3302}) \\ k_{12}^{\sigma} &= D_3(\sigma_{xx}^{\mathrm{dev}}\lambda_{1111} + \sigma_{yy}^{\mathrm{dev}}\lambda_{2211} + \sigma_{zz}^{\mathrm{dev}}\lambda_{3311}) \\ k_{21}^{\sigma} &= D_4(\sigma_{xx}^{\mathrm{dev}}\lambda_{1111} + \sigma_{yy}^{\mathrm{dev}}\lambda_{2211} + \sigma_{zz}^{\mathrm{dev}}\lambda_{3311}) \end{aligned} \tag{15}$$

Among these equations, K and D are parameters that need to be identified from measurements.

When stress is applied, the new pinning field $h_{\mathrm{ir}\text{-}\sigma}$ is

$$h_{\mathrm{ir}\text{-}\sigma} = \frac{\|\boldsymbol{k}\boldsymbol{\theta}_{\mathrm{ir}}\|}{\|\boldsymbol{k}_0\boldsymbol{\theta}_{\mathrm{ir}}\|}h_{\mathrm{ir}} \tag{16}$$

where $\boldsymbol{\theta}_{\mathrm{ir}}$ is the direction of $\boldsymbol{h}_{\mathrm{ir}}$.

For one hysteron, its reversible effective field $\boldsymbol{h}_{\text{re-eff}}$ at current calculation step is updated by (17) with respect to $\boldsymbol{h}'_{\text{re-eff}}$ at previous calculation step

$$\boldsymbol{h}_{\text{re-eff}} = \begin{cases} \boldsymbol{h}'_{\text{re-eff}}, & \left|\boldsymbol{H}_{\text{eff}} - \boldsymbol{h}'_{\text{re-eff}}\right| < h_{\text{ir}\text{-}\sigma} \\ \boldsymbol{H}_{\text{eff}} - h_{\text{ir}\text{-}\sigma}\dfrac{\boldsymbol{H}_{\text{eff}} - \boldsymbol{h}'_{\text{re-eff}}}{\left|\boldsymbol{H}_{\text{eff}} - \boldsymbol{h}'_{\text{re-eff}}\right|}, & \left|\boldsymbol{H}_{\text{eff}} - \boldsymbol{h}'_{\text{re-eff}}\right| \geq h_{\text{ir}\text{-}\sigma} \end{cases} \tag{17}$$

Then the outputs of N_{h} hysterons are summed to obtain the total reversible field $\boldsymbol{H}_{\text{re-eff}}$ by the probability densities function of the pinning field.

$$\boldsymbol{H}_{\text{re-eff}} = \sum_{n=1}^{N_{\mathrm{h}}} \boldsymbol{h}_{\text{re-eff}}^n \cdot p(h_{\mathrm{ir}}^n). \tag{18}$$

The amplitude of magnetization M is calculated by a function with respect to $H_{\text{re-eff}}$ to characterize the anhysteretic curve of the sample. Under rotational magnetization, the coherent rotation should be considered to make sure that the rotational loss drops when the sample is close to saturation. Therefore, the angle of magnetization should contain the effects of angle of $\boldsymbol{H}_{\text{re-eff}}$ and angle of $\boldsymbol{H}_{\text{eff}}$ at the same time. The above calculation processes correspond to equation (11) and (17) in [7], respectively.

In summary, the proposed model is an extended version of the anisotropic hysteresis model in [7] for multiaxial stress condition, the overall identification and calculation process of the two models is consistent. Due to limitation of paper length, it will not be introduced in this paper.

III. Application

The non-oriented electrical steel sheets M400-50A is utilized to verify the presented model. The rotational magnetic properties are measured at a controlled waveform and frequency of the magnetic flux density of 10 Hz. The rolling direction (RD) of the sample is along the *x*-axis and the transverse direction (TD) is along the *y*-axis. A detailed description of the measurement setup and the approach followed hereinafter is given in [11]. Data with B_{p} = 1.2 T are used for identification in this paper to verify the capacity of proposed the model for modeling anisotropy and loss under multiaxial stress.

A. Identification

In (11), due to the presence of λ in $\boldsymbol{H}_{\sigma}$, the value range of function G can be set to 0-1. The g parameters contained in function G are determined using the relationship between the per unit value of magnetostrictive strain and magnetization in Fig.4 of [8]. For other parameters, parameters related to anisotropic hysteresis model are identified first by the measurements without stress, then parameters related to magneto-mechanical behaviors are identified by the measurements under multiaxial stress, as shown in Table I. The parameters not introduced in this article and the definition of error function can be found in reference [7]. The fitting errors for the two types of measurements are 10.7 % and 3.28 %, respectively.

TABLE I
Parameters of Proposed Model

Name	Unit	Value
a_1	A/m	50.7
a_2	A/m	7.0
M_{s}	MA/m	1.0
ω	-	4.4×10^{-1}
K_{40}	J/m^3	149.9
K_{04}	J/m^3	–147.9
K_{22}	J/m^3	47.2
K_{40}	J/m^3	–41.3
K_{40}	J/m^3	59.2
K_{40}	J/m^3	29.2
K_{40}	J/m^3	43.1
k_{12}^0	J/m^3	7.3×10^{-2}
k_{21}^0	J/m^3	8.7
k_{22}^0	J/m^3	9.7
k_{ani}	-	-4.8×10^{-3}
η	-	9.8×10^{-1}
C_1	A/m	6.0
C_2	A/m	177.1

(a) No-stress parameters

Name	Unit	Value
λ_{1120}	μm/m	1.5
λ_{1102}	μm/m	–3.5
λ_{1111}	μm/m	7.9×10^{-1}
λ_{2220}	μm/m	-7.5×10^{-1}
λ_{2202}	μm/m	2.7
λ_{2211}	μm/m	-5.0×10^{-1}
q_1	-	2.6
q_2	MPa	15.2
q_3	MPa	37.1
D_1	-	3.2×10^{-2}
D_2	-	-8.1×10^{-3}
D_3	-	9.8×10^{-2}
D_4	-	5.4×10^{-2}
g_1	-	4.8×10^{-1}
g_3	-	2.3×10^{-1}
g_5	-	-0.7×10^{-1}

(b) Stress parameters

B. Validation

Fig. 1 shows the comparison between measured and calculated rotational magnetic properties under uniaxial stress applied along RD. It can be seen that the influence of stress on

vector magnetic properties is more apparent in one direction. Overall, stress has a certain impact on the coercivity field, with larger values indicating greater coercivity, but the impact is relatively small. Therefore, the pinning field related coefficients D_1~D_4 are relatively small. Compared with the measured results, the predicted results have good consistency in overall trend, while the predicted trajectory is smoother.

Fig. 2 shows the comparison between measured and calculated vector magnetic properties under multiaxial stress. The vector magnetic properties predicted by the proposed model are consistent with measurements in terms of the trend of stress variation. However, there are significant differences in the shape of the trajectory. What's more, the maximum error of rotational losses is 13.8 % and the mean error is 3.4%.

Fig. 3 shows the comparison between the measured and calculated rotational losses under different stress configurations. In Fig. 3(a), measured stress configurations are shown by dot markers and losses of other stress configurations come from interpolation. It is proved that the proposed model exhibits good consistency in the trend of rotational losses with stress variation.

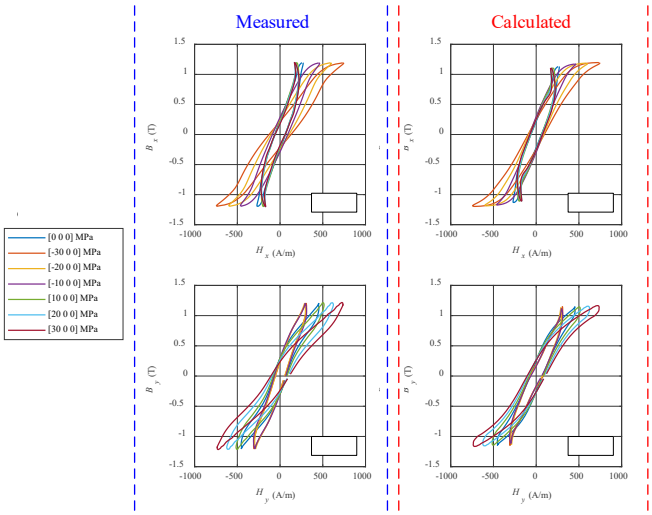

Fig. 1. Comparison between measured and calculated rotational magnetic properties under uniaxial stress applied along RD (B_p = 1.2 T).

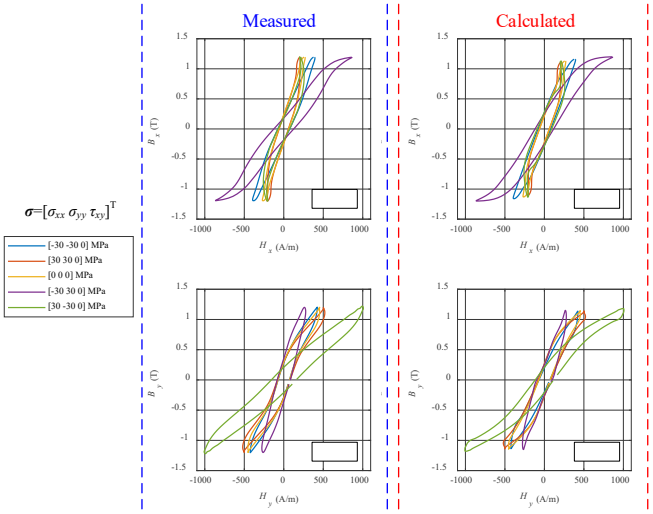

Fig. 2. Comparison between measured and calculated vector magnetic properties under biaxial stress (B_p = 1.2 T).

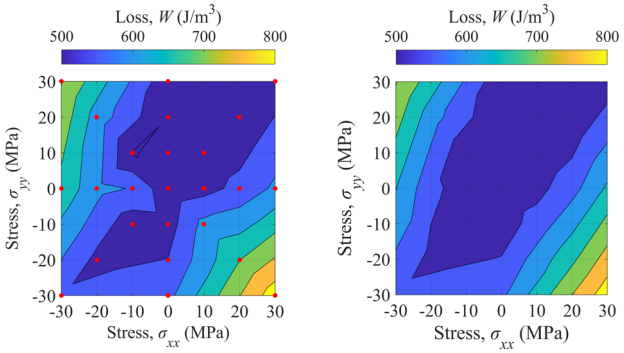

(a) Measured losses (b) Calculated losses

Fig. 3. Comparison between the measured and calculated rotational losses under different stress conditions (B_p = 1.2 T).

IV. Conclusion

This paper extends the anisotropic vector hysteresis model to a vector hysteresis model under multiaxial stress. Based on the crystal energy and the coordinate transformation, the transformation from microscopic to macroscopic magneto-elastic properties of sample is achieved. Combined with the typical characteristics of magnetostriction coefficient, the expression of stress field is derived, then the effective field which can predict the vector anhysteretic magnetic properties under stress is obtained. The effective field is used as input of EB model and the hysterons of EB model is modified to vary with energy. The accuracy of the proposed model is verified by the measured rotational magnetic properties under different multiaxial stress conditions. In fact, although magnetostrictive measurements are not involved in the identification process, magnetostrictive properties can still be predicted, which will be carried out in future work.

Acknowledgment

This work was supported in part by the National Natural Science Foundation of China under Grant 52130710, in part by the Funds for Creative Research Groups of Hebei Province under Grant E2020202142, in part by the "S&T" Program of

Hebei under Grant 20311801D. F. Martin and A. Belahcen acknowledge the funding from the Academy of Finland under grant 346438.

REFERENCES

[1] K. Yamazaki, H. Takeuchi. “Impact of mechanical stress on characteristics of interior permanent magnet synchronous motors,” IEEE Trans. Ind. Appl. vol. 53, no. 2, pp. 963-970, Oct. 2016.

[2] L. Daniel and O. Hubert. “An equivalent stress for the influence of multiaxial stress on the magnetic behavior,” J. Appl. Phys., vol. 105, no. 7, Art. No. 07A313, Apr. 2009.

[3] M. Gueye, F. Zighem, M. Belmeguenai, et al. “Ferromagnetic resonance in thin films submitted to multiaxial stress state: application of the uniaxial equivalent stress concept and experimental validation,” J. Phys. D. Appl. Phys., vol. 49, no. 26, Art. No. 265001, May. 2016.

[4] L. Daniel, O. Hubert, N. Buiron, hand R. Billardon, “Reversible magnetoelastic behavior: A multiscale approach,” J. Mech. Phys. Solids., vol. 56, no. 3, pp. 1018–1042, Mar. 2008.

[5] L. Daniel, M. Rekik, O. Hubert. “A multiscale model for magneto-elastic behaviour including hysteresis effects,” Arch. Appl. Mech., vol. 84, pp. 1307-1323, May. 2014.

[6] D. Vanoost, S. Steentjes, J. Peuteman, et al. “Multiscale and macroscopic modeling of magneto‐elastic behavior of soft magnetic steel sheets,” Int. J. Numer. Model.: Electron. Netw. Devices Fields, vol. 31, no. 2, pp. 1-9, Apr. 2017.

[7] R. Chen, F. Martin, Y. Li, et al. “An energy-based anisotropic vector hysteresis model for rotational electromagnetic core loss,” IEEE Trans. Ind. Electron., vol. 71, no. 6, pp. 6084-6094, Jun. 2024.

[8] D. Singh, F. Martin, P. Rasilo, et al. “Magnetomechanical model for hysteresis in electrical steel sheet,” IEEE Trans. Magn., vol. 52, no. 11, Art. No. 7301109, Nov. 2016.

[9] F. Henrotte, A. Nicolet, and K.Hameyer, “An energy-based vector hysteresis model for ferromagnetic materials,” COMPEL Int. J. Comput. Math. Elect. Electron. Eng., vol. 25, no. 1, pp. 71–80, Jan. 2006.

[10] F. Martin, R. Chen, J. Taurines, et al. “Anisotropic hysteresis representation of steel sheets based on a vectorization technique applied to Jiles-Atherton model,” IEEE Trans. Magn., vol. 60, no. 3, Art. No. 7300504, Mar. 2024.

[11] U. Aydin, F. Martin, P. Rasilo, et al. “Rotational single sheet tester for multiaxial magneto-mechanical effects in steel sheets,” IEEE Trans. Magn., vol. 55, no. 3, Art. No. 2001810, Mar. 2019.